Eur J Nucl Med Mol Imaging (2016) 43:1115–1123
DOI 10.1007/s00259-015-3274-4

ORIGINAL ARTICLE

Reproducibility of O-(2-^{18}F-fluoroethyl)-L-tyrosine uptake kinetics in brain tumors and influence of corticoid therapy: an experimental study in rat gliomas

Carina Stegmayr[1] · **Michael Schöneck**[1] · **Dennis Oliveira**[1] · **Antje Willuweit**[1] · **Christian Filss**[1,2] · **Norbert Galldiks**[1,3] · **N. Jon Shah**[1,2,4] · **Heinz H. Coenen**[1,2] · **Karl-Josef Langen**[1,2]

Received: 11 August 2015 / Accepted: 27 November 2015 / Published online: 8 December 2015

Abstract
Purpose Positron emission tomography (PET) using O-(2-^{18}F-fluoroethyl)-L-tyrosine (^{18}F-FET) is a well-established method for the diagnostics of brain tumors. This study investigates reproducibility of ^{18}F-FET uptake kinetics in rat gliomas and the influence of the frequently used dexamethasone (Dex) therapy.
Methods F98 glioma or 9L gliosarcoma cells were implanted into the striatum of 31 Fischer rats. After 10–11 days of tumor growth, the animals underwent dynamic PET after injection of ^{18}F-FET (baseline). Thereafter, animals were divided into a control group and a group receiving Dex injections, and all animals were reinvestigated 2 days later. Tumor-to-brain ratios (TBR) of ^{18}F-FET uptake (18–61 min p.i.) and the slope of the time-activity-curves (TAC) (18–61 min p.i.) were evaluated using a Volume-of-Interest (VOI) analysis. Data were analyzed by two-way repeated measures ANOVA and reproducibility by the intraclass correlation coefficient (ICC).
Results The slope of the tumor TACs showed high reproducibility with an ICC of 0.93. A systematic increase of the TBR in the repeated scans was noted (3.7±2.8 %; $p<0.01$), and appeared to be related to tumor growth as indicated by a significant correlation of TBR and tumor volume ($r=0.77$; $p<0.0001$). After correction for tumor growth TBR showed high longitudinal stability with an ICC of 0.84. Dex treatment induced a significant decrease of the TBR (−8.2±6.1 %; $p<0.03$), but did not influence the slope of the tumor TAC.
Conclusion TBR of ^{18}F-FET uptake and tracer kinetics in brain tumors showed high longitudinal stability. Dex therapy may induce a minor decrease of the TBR; this needs further investigation.

Keywords PET · Brain tumors · O-(2-[^{18}F]fluoroethyl)-L-tyrosine (FET) · Reproducibility · Dexamethasone treatment · Rat glioma model

Electronic supplementary material The online version of this article (doi:10.1007/s00259-015-3274-4) contains supplementary material, which is available to authorized users.

✉ Karl-Josef Langen
k.j.langen@fz-juelich.de

Carina Stegmayr
c.stegmayr@fz-juelich.de

[1] Research Center Jülich, Institute of Neuroscience and Medicine, Jülich, Germany

[2] Department of Nuclear Medicine and Neurology, University of Aachen, Aachen, Germany

[3] Department of Neurology, University of Cologne, Cologne, Germany

[4] Jülich-Aachen Research Alliance (JARA) – Section JARA-Brain, Jülich, Germany

Introduction

Positron emission tomography (PET) using the amino acid O-(2-^{18}F-fluoroethyl)-L-tyrosine (^{18}F-FET) is a rapidly spreading method for brain tumor diagnostics due to logistic advantages of F-18 labelling (half-life 109.8 min) compared with L-[methyl-^{11}C]-methionine (^{11}C-MET) PET [1–4]. Multiple studies have proven the clinical value of ^{18}F-FET PET to determine the extent of cerebral gliomas for treatment planning, biopsy guidance, detection of tumor recurrences, prognosis, and treatment monitoring [5–11]. Furthermore, dynamic ^{18}F-FET PET may provide additional information about the grading of gliomas [12–15]. Thus, continuously

increasing ^{18}F-FET uptake is a typical finding in low-grade gliomas, while kinetics with an early peak of ^{18}F-FET uptake within the first 20 min after injection followed by a washout indicates a high-grade glioma.

Data on the reproducibility of radiolabeled amino acid uptake in tumors are rare. A recent study demonstrated acceptable reproducibility of anti-1-amino-3-^{18}F-fluorocyclobutane-1-carboxylic acid uptake in prostate cancer, but the time interval between the studies in that retrospective study was variable [16]. Using the tyrosine analogue ^{123}I-iodo-α-methyltyrosine, a maximal deviation of the tumor-to-brain ratio (TBR) of 5 % has been observed in repeated studies before and after infusion of competing amino acids, indicating that the TBR of amino acid uptake in gliomas is a rather stable parameter [17]. Previous studies have assumed changes of the TBR of ^{18}F-FET uptake during therapy monitoring of more than 10 % as significant [18]. Up to now, the reproducibility of ^{18}F-FET kinetics, however, has not yet been assessed.

Another important aspect in repeated ^{18}F-FET PET scans of brain tumors is the potential influence of dexamethasone (Dex) treatment on tracer uptake. Dex treatment is the current standard therapy for patients suffering from brain edema, as it rapidly restores brain homeostasis and the integrity of the blood-brain barrier (BBB), and thus reduces symptoms [19, 20]. A previous study reported that corticosteroid treatment moderately reduced ^{11}C-MET uptake in high-grade gliomas [21].

The purpose of this experimental study was to investigate the reproducibility of ^{18}F-FET uptake and tracer kinetics in two different rat glioma models, and in addition, to explore the influence of Dex therapy.

Materials and methods

Animals

Thirty-one male Fischer-344 rats (Charles River Laboratories), weighing between 250 and 310 g were included in this study. The animals were kept under standard housing conditions with free access to food and water. In all animals, the presence of a brain tumor was verified by histological staining after completion of the PET studies. All animal experiments were carried out in conformance with the German Protection of Animals Act and with a permit from the local Animal Protection Committee.

Cell culture and tumor inoculation

F98 cells (ATCC® # CRL-2397™; LGC Standards GmbH) were cultured as described previously [22]. 9L cells (ECACC GS-9L) were cultured in minimum essential medium Eagle (MEM) supplemented with 10 % FCS, Pen/Strep, glutamate and 1 % non-essential amino acids (NEAA). At confluence of ~95 %, cells were prepared for inoculation: cells were washed twice with PBS and detached by incubating with trypsin/EDTA for ~5 min. F98 and 9L cells were resolved in growth medium to a concentration of 30,000 cells/5 μl and 65,000 cells/5 μl, respectively.

F98 and 9L rat glioma cells were stereotactically implanted into the right basal ganglia under anesthesia as described previously [23]. F98 tumors were allowed to grow for 11 days (d) and 9L tumors for 10 days prior to the first PET scan. This period was found to be optimal for the respective tumor model in order to obtain sufficient tumor size for PET measurements without the animals suffering from major neurological deficits.

Grouping and Dex treatment

Rats were grouped to test the stability of ^{18}F-FET accumulation (F98 glioma: n=10; 9L gliosarcoma: n=8) on the one hand, and influence of Dex treatment (F98: n=6; 9L: n=7) on the other. For testing reproducibility or longitudinal stability, respectively, rats underwent baseline and control FET PET scans in intervals of 48 h without intermediate treatment. To test the influence of treatment with Dex, rats were injected intraperitoneally (i.p.) with a dose of 8 mg/kg Dex (Dexa 8 mg inject, Jenapharm®, mibe GmbH). Dosage of Dex was based on previous literature [24]. Dex was applied immediately after baseline ^{18}F-FET PET, followed by two further injections of 4 mg/kg Dex i.p. after 24 and 48 h. Control ^{18}F-FET PET was done 90 min after the last Dex application.

PET studies

At the time of the PET scans, the rats had fasted for at least 12–16 h. After isoflurane anaesthetization, a venous catheter was inserted into one tail vein and fixed to the rat's tail with superglue. The rats were positioned in the field-of-view of the small animal Siemens INVEON scanner (Siemens-CTI) [25]. Body temperature was maintained at 37.8±0.3 °C with an infrared lamp. Breathing rate was controlled with a pressure sensitive pad positioned under the rats and was regulated between 48 and 55 bpm. ^{18}F-FET was synthesized in-house as described elsewhere with a specific radioactivity of >200 GBq/μmol [26]. After a transmission scan (10–20 min), dynamic data acquisition was performed in three-dimensional (3D) list mode for 61 min starting with injection of 40±3 MBq ^{18}F-FET in saline into the tail vein (bolus injection of 0.5 ml in 1 min). Emission data were framed into a dynamic sequence of 6×10 s, 5×60 s, 5×3 min, 10×4 min frames. Filtered back-projection (Ramp filter, cutoff=0.5) was applied to reconstruct 159 slices with an image voxel size of 0.7764×0.7764×0.796 mm^3 (matrix size: 128×128×159). Images were corrected for random coincidences, scatter radiation and attenuation. After the second PET scan, rats were sacrificed, brains were removed, quickly frozen in liquid isopentane (−50 °C) and cut into 20 μm thick slices with a cryostat. Presence of a brain tumor was verified by fluorescence staining with 40,6-

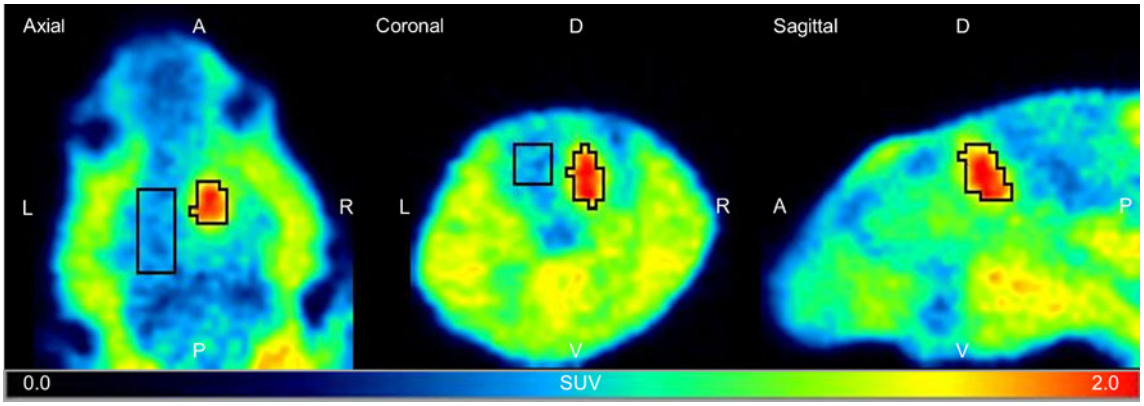

Fig. 1 Summed PET images (18–61 min p.i.) of ^{18}F-FET uptake in a 9L gliosarcoma (transversal slice on the *left*, coronal slice in the center and sagittal slice on the *right*). The *black lines* indicate the tumor VOI and the reference VOI in the contralateral hemisphere

diamidino-2-phenylindole dihydrochloride (DAPI; nuclear stain).

In order to test the effect of Dex treatment on the permeability of the blood-tumor barrier, two rats of each subgroup were injected i.v. with 500 μl/kg 2 % Evans blue in NaCl 30 min prior to sacrifice. Evans blue fluorescence in the tumor bearing brain slices was evaluated quantitatively using an Aida Image Analyzer (AIDA Version 4.50; Raytest-Fuji).

Data analysis

Analysis of PET data was performed with Pmod Version 3.4 (PMOD Technologies Ltd). ^{18}F-FET uptake in the tissue was expressed as standardized uptake value (SUV) by dividing the radioactivity (kBq/ml) in the tissue by the radioactivity injected per gram of body weight. Summed PET images (18–61 min p.i.) were used for volume of interest (VOIs) analysis. The tumor VOI on ^{18}F-FET PET scans was determined by a 3D autocontouring process using a cutoff for the TBR of ^{18}F-FET uptake of>1.7 yielding a tumor size similar to that in autoradiography for 9L gliomas. ^{18}F-FET uptake in the unaffected brain tissue was determined by a larger VOI placed in the contralateral hemisphere in an area of normal brain tissue including white and gray matter (250 voxels, 120 mm^3). An example of VOI positioning in a 9L gliosarcoma is shown in Fig. 1. After Dex treatment, an elevated ^{18}F-FET uptake in the normal brain tissue was noted, resulting in falsely too small tumor VOIs. In order to overcome this systematical error, the autocontouring process after Dex treatment was based on ^{18}F-FET brain uptake in the baseline scan using a cutoff of>1.7, which yielded correct tumor sizes compared with autoradiography. TBR was calculated by dividing the mean VOI value (Bq/ml) of the tumor by the mean VOI value of normal brain tissue. Time-activity curves (TACs) were generated by application of these VOIs to the entire dynamic data set. In order to quantify the slope of the curve in the late phase of ^{18}F-FET uptake, a linear regression line was fitted to the late phase of the curves (18–60 min p.i.).

Statistics

Descriptive statistics are provided as mean and standard deviation (SD). Two-way repeated measures (TW RM) ANOVAs were performed to detect differences in the longitudinal test for stability, in the Dex treatment study, and between the different tumor models without correction for multiple testing.

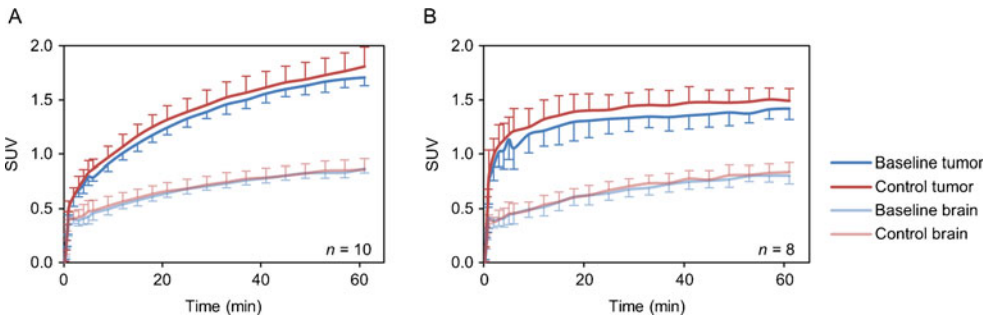

Fig. 2 Longitudinal test for stability: Time-activity curves of ^{18}F-FET uptake in tumor and brain of F98 glioma (**a**) and 9L glioma bearing rats (**b**). The *blue curves* represent the baseline scan and the *red curves* the control scan (mean values±SD; one-sided SD for better illustration). There is a significantly higher ^{18}F-FET uptake in the tumors in the control scans due to tumor growth, but the shape of the curves remains identical. Brain TACs show perfect overlay in both tumor models. Note that F98 and 9L gliomas exhibit essentially different ^{18}F-FET kinetic patterns indicating tumor type specific ^{18}F-FET transport

Table 1 Results of longitudinal test for stability

Parameter	Baseline	Control	*p* value
F98 Glioma (*n*=10)			
SUV Tumor (18–61 min p.i.)	1.50±0.08	1.58±0.15	n.s. (0.09)
SUV Brain (18–61 min p.i.)	0.76±0.05	0.77±0.08	n.s. (0.32)
Tumor/ Brain (18–61 min p.i.)	1.98±0.07	2.04±0.06	0.002
Slope Tumor [SUV/h]	0.76±0.10	0.72±0.11	n.s. (0.30)
Slope Brain [SUV/h]	0.33±0.05	0.33±0.05	n.s. (0.43)
Tumor Volume [mm^3]	55.61±25.32	109.06±44.54	<0.001
9L Gliosarcoma (*n*=8)			
SUV Tumor (18–61 min p.i.)	1.36±0.12	1.46±0.13	0.037
SUV Brain (18–61 min p.i.)	0.73±0.07	0.75±0.08	n.s. (0.32)
Tumor/ Brain (18–61 min p.i.)	1.87±0.07	1.95±0.09	<0.001
Slope Tumor	0.17±0.12	0.17±0.13	n.s. (0.90)
Slope Brain	0.29±0.03	0.32±0.04	n.s. (0.43)
Tumor Volume [mm^3]	22.79±10.21	49.24±2.19	0.004

The reliability of PET parameters, i.e. TBR and tumor slope, was tested by computing Pearson's correlation coefficients and interclass correlation coefficients (ICCs). We considered values between 0.80 and 1.00 as very high correlation. Furthermore, Bland-Altman analysis was used for evaluation of the differences in TBR and tumor slope in the stability study. *p* values of 0.05 or less were considered significant. Systematic divergence of parameters from perfect stability in the 2 days longitudinal setup were analyzed by least squares regression analysis in which the slope and intercept can be used to determine agreement [27]. The amount of y-intercept different from zero indicates a constant systematic error between baseline and control study. Statistical analysis was performed using SigmaPlot for Windows, Version 12.0 and, for the ICC, IBM SPSS Statistics for Windows, Version 22.

Results

Reproducibility

TACs of ^{18}F-FET uptake in tumor and brain of F98 glioma and 9L glioma bearing rats in baseline and control PET studies are shown in Fig. 2. ^{18}F-FET uptake in the F98 and 9L tumors was significantly higher in the control scan than in the baseline scan (TBR F98: 2.04±0.06 vs. 1.98±0.07, n=10, p=0.002; TBR 9L: 1.95±0.09 vs. 1.87±0.07, n=8, p<0.001) (Table 1). There was a significant correlation between TBR and tumor volume (Fig. 3, r=0.77; p<0.0001) indicating that the rising TBR was related to tumor growth during the 2-day interval (Fig. 3). Accordingly, TBR of both tumor models in baseline and control studies showed a significant correlation but a systematic deviation from the line of unity (r=0.81, p<0.0001, n=18, Fig. 4a). Least square correlation analysis yielded a slope close to unity (0.78) with a y-axis intercept of 0.48 indicating a systematic error induced by tumor growth during the 2 days interval [27].

Therefore, for calculation of the ICC, TBR values of control studies were corrected for tumor growth by subtracting the mean increase of TBR between baseline and control study from that of the control study, which yielded an ICC of 0.84, indicating a high longitudinal stability of TBR in this experimental setup (Fig. 5a).

The shape and slope of the TACs of both tumor models were highly reproducible, as they showed no significant difference between baseline and control PET studies. Also, the TACs of ^{18}F-FET uptake in the normal brain revealed excellent overlay in both tumor models in baseline and control PET studies and SUV of ^{18}F-FET uptake, and the slope of the TAC

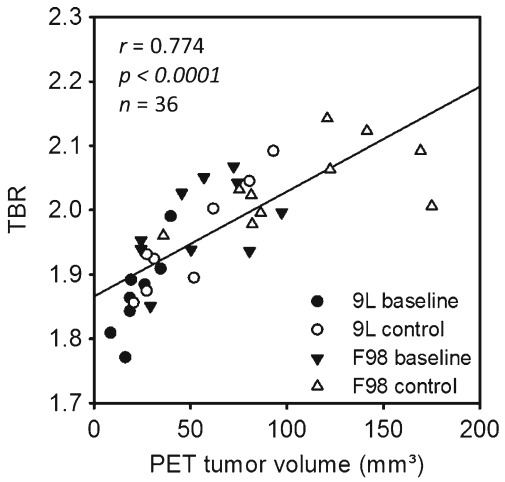

Fig. 3 Correlation of TBR of FET uptake and tumor volume as determined by PET at baseline (*black symbols*) and at control (*white symbols*). Data of 9L gliomas are indicated by *circles* and data of 9L gliomas by *triangles*. There is significant increase of TBR with increasing tumor volume

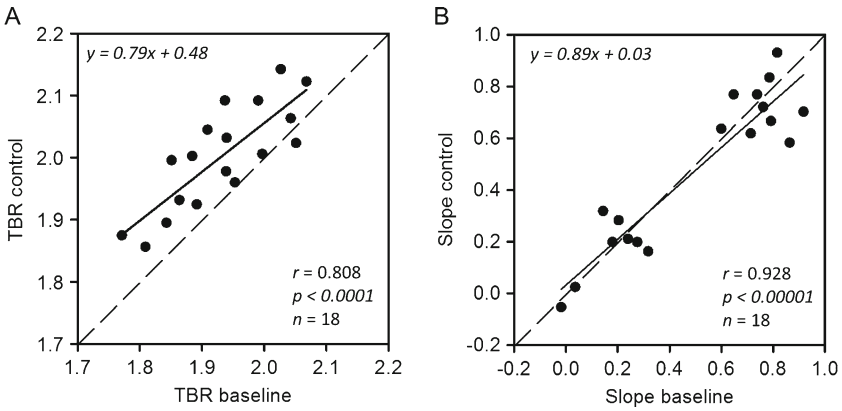

Fig. 4 Correlation of TBR (**a**) and slope of the TAC (**b**) of both tumor models in the baseline and control study. Both parameters showed a significant correlation, but for TBR, a deviation from the line of unity (*dashed line*) with a y-axis intercept of+0.48 was observed, indicating a systematic error that is assumed to be caused by tumor growth (see Fig. 3)

in the brain exhibited no significant differences between baseline and control PET studies. The slope of both tumor models in baseline and control studies showed a significant correlation (Fig. 4b) (r=0.93, p<0.00001, n=18). The ICC was 0.93, indicating very high reproducibility of slope (Fig. 5).

When comparing the TAC of ^{18}F-FET uptake in the different tumor models, significant differences were noted (Fig. 2). Thus, ^{18}F-FET uptake in F98 and 9L rat gliomas showed significant differences for tumor SUV (1.54±0.03 vs. 1.41± 0.04, p=0.014), TBR (2.01±0.02 vs. 1.91±0.02, p=0.005) and tumor slope (0.74±0.03 vs. 0.17±0.03, p<0.001), indicating a tumor type specific transport of ^{18}F-FET.

Dexamethasone treatment

The TACs of ^{18}F-FET uptake in tumor and brain of F98 glioma and 9L glioma-bearing rats in the baseline and control scans after Dex treatment are shown in Fig. 6. After Dex treatment, a slight increase of the SUV of ^{18}F-FET uptake in the brain was observed, leading to a significant decrease of the TBR in both models (Table 2). Dex treatment induced a decrease of the TBR of ^{18}F-FET uptake of - 4.6±6.1 % in F98 gliomas (p=0.03) and of - 11.3±4.2 % in 9L gliomas (P<0.001). All other parameters were not significantly influenced by Dex treatment. The TBR and slope of ^{18}F-FET uptake in both tumor models in baseline and control studies after Dex treatment showed a significant correlation (Fig. 7) (r=0.94; p<0.00001 and r=0.87, p<0.0001; n=13).

Representative pictures demonstrating the effectiveness of Dex treatment on Evans blue extravasation in the different tumor models are presented in Fig. 8. In F98 gliomas of Dex treated rats, Evans blue fluorescence was approximately 50 % lower than in tumors of untreated rats indicating a significant effect of Dex treatment on the permeability of the blood-tumor barrier. In 9L gliomas, the effect was even more pronounced, leading to a reduction of Evans blue fluorescence of approximately 90 % in comparison to 9L gliomas of untreated rats (Fig. 8).

Discussion

The purpose of this study was to evaluate the reproducibility of ^{18}F-FET uptake and kinetics in brain tumors. ^{18}F-FET PET has been used in several studies to assess response to treatment in humans [5, 18, 28–31] and also in animal models [32, 33]. These studies were based mainly on the evaluation of the TBR of ^{18}FET uptake, but recent studies have also highlighted the

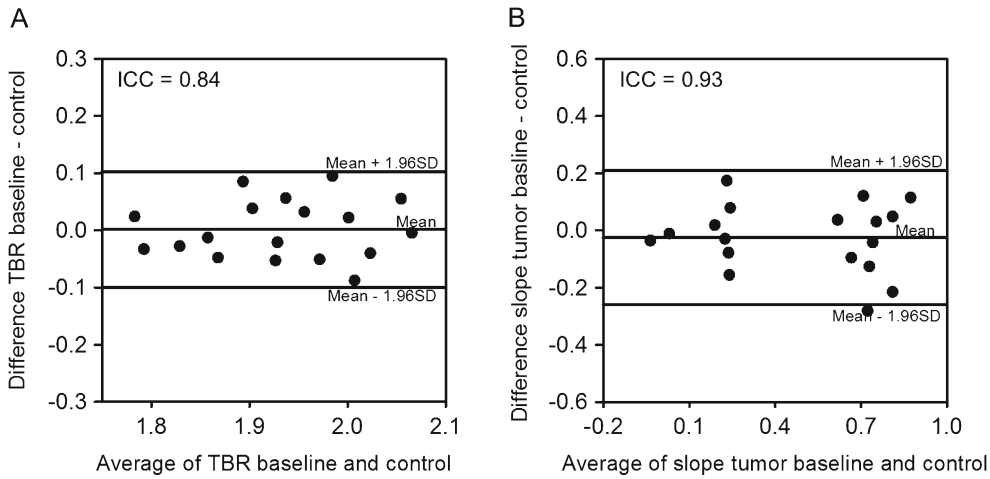

Fig. 5 Bland- Altman plots of TBR (after correction for tumor growth) (**a**) and slope of the TAC in tumors (**b**). *Lines* show combined mean and 95 % confidence interval. The ICC showed high values indicating very high stability

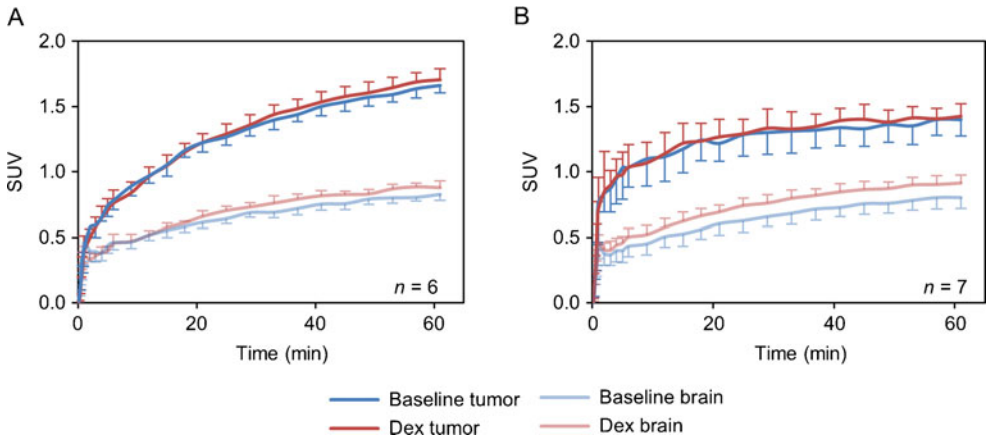

Fig. 6 Dex study: Time-activity curves of ^{18}F-FET uptake in tumor and brain of F98 glioma (**a**) and 9L glioma bearing rats (**b**). The *blue curves* represent the baseline scan and the *red curves* the control scan after Dex treatment (mean values±SD; one-sided SD for better illustration). After Dex treatment, a slight increase of ^{18}F-FET uptake in the brain was observed, leading to a significant decrease of the TBR in both models. ^{18}F-FET kinetics in the tumors is not significantly influenced by Dex treatment. Again, F98 and 9L gliomas exhibit essentially different ^{18}F-FET kinetics, indicating tumor-type-specific ^{18}F-FET transport

role of altered ^{18}F-FET kinetics during follow-up to identify malignant transformation of low-grade gliomas or during brachytherapy of recurrent glioblastoma to detect tumor response [34, 35]. For the definition of objective criteria by which an alteration can be considered significant, the within-patient reproducibility of the TBR and curve pattern of ^{18}F-FET uptake must be known and up to date, this issue has not yet been addressed adequately.

The results of this experimental study demonstrated a significant correlation of TBR in the baseline and control study, but there was a slight but significant increase of the TBR in the control study in both tumor models. The regression line showed a positive parallel shift in comparison to the line of unity, suggesting a systematic error (Fig. 4a). The analysis of the relationship between TBR and tumor volume in PET showed a significant correlation, indicating that the rising TBR was related to tumor growth during the 2-day interval (Fig. 3). One possible explanation for the increase of the TBR is an increase in metabolic activity in the tumors within the interval of 2 days, but the difference can also be explained by technical reasons in this experimental setup. Since the spatial resolution of the animal PET is relatively poor in relation to tumor size, the apparent increase in tumor uptake may also be caused by a decreasing influence of the partial volume effect with increasing tumor size, which leads to higher tumor values. Regardless of the cause of the systematic error, after correction for tumor growth, TBR between baseline and control study yielded an ICC of 0.84, indicating a high longitudinal stability of TBR. Even without correction, the deviation of TBR between baseline and control was only 4.4±2.0 %. Thus,

Table 2 Results of dexamethasone study

Parameter	Baseline	Dex[a]	*p* value
F98 Glioma (*n*=6)			Dex vs. baseline
SUV Tumor (18–61 min p.i.)	1.44±0.06	1.55±0.08	n.s. (0.14)
SUV Brain (18–61 min p.i.)	0.73±0.04	0.78±0.03	n.s. (0.13)
Tumor/ Brain (18–61 min p.i.)	1.99±0.10	1.89±0.15	0.03
Slope Tumor [SUV/h]	0.69±0.08	0.78±0.08	n.s. (0.51)
Slope Brain [SUV/h]	0.33±0.02	0.37±0.04	n.s. (0.27)
Volume [mm^3]	69.33±38.98	117.07±58.07	<0.001
9L Gliosarcoma (*n*=7)			
SUV Tumor (18–61 min p.i.)	1.32±0.14	1.50±0.10	n.s. (0.11)
SUV Brain (18–61 min p.i.)	0.71±0.08	0.82±0.06	<0.001
Tumor/ Brain (18–61 min p.i.)	1.86±0.03	1.65±0.08	<0.001
Slope Tumor	0.22±0.11	0.19±0.03	n.s. (0.66)
Slope Brain	0.33±0.03	0.35±0.03	n.s. (0.35)
Volume [mm3]	21.59±11.79	46.68±23.04	0.002

[a] Tumor VOIs based on an auto-contouring process using SUV brain of the baseline scan for cutoff >1.7

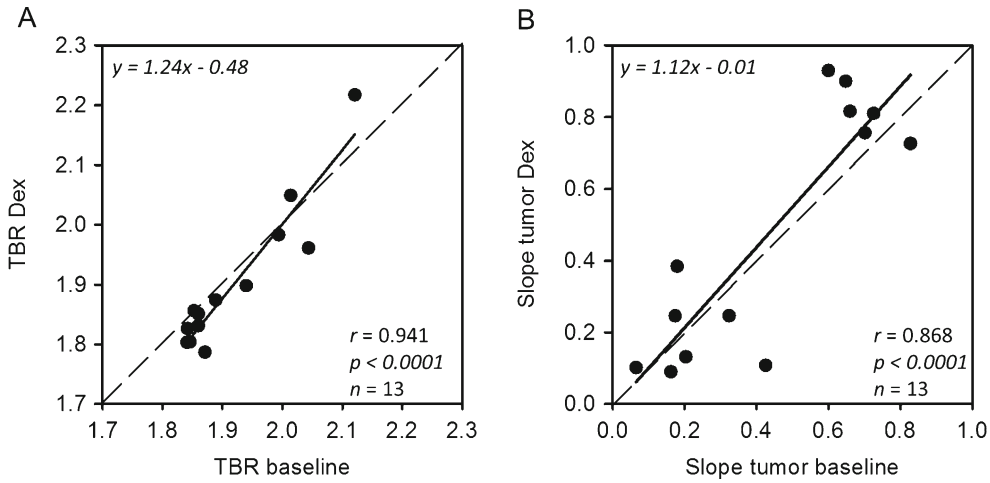

Fig. 7 Correlation of TBR (**a**) and slope of the TACs (**b**) of both tumor models in the baseline and control scan after Dex treatment (*dashed line* indicates line of unity). Again, both parameters showed a significant correlation

a threshold of 10 %, which was used in former studies to identify tumor response, would be sufficient to rule out physiological and methodological variation [18].

The comparison of curve patterns and ^{18}FET-uptake in the tumors in the baseline and control study showed high reproducibility, with a significant correlation of slopes and an ICC of 0.93 (Figs. 2, 4b, and 5b).

Another interesting finding in this study is the different shape of the TAC of ^{18}F-FET uptake in the F98 glioma compared with the 9 L gliosarcoma model, which showed high reproducibility in the longitudinal test for stability and after Dex treatment (Figs. 2 and 6). This finding supports the hypothesis that the shape of the TAC of ^{18}F-FET uptake is in fact a parameter characterizing the biological properties of a tumor. As outlined above, ^{18}F-FET kinetics may provide interesting additional information on tumor grade and may change during malignant transformation and after therapy [11–15, 34, 35]. A recent study has shown that ^{18}F-FET is trapped within human glioblastoma cells due to the asymmetry of its intra- and extracellular recognition by the system L transporter LAT1 [36]. It is tempting to speculate that differences of ^{18}F-FET transport asymmetry in the two tumor models are responsible for the different uptake curves.

The second important aspect of this study was to investigate the effect of corticosteroid treatment on ^{18}F-FET uptake and kinetics in brain tumors. As already mentioned above, Dex treatment is the current standard therapy for patients suffering from brain edema and is frequently used in brain tumor patients during the course of disease. Therefore, it can happen that a patient at repeated investigations by ^{18}F-FET PET is once treated with Dex and once not. The results of this study demonstrate that the effect of Dex treatment on ^{18}F-FET uptake and kinetics in gliomas is small. A mean decrease of the TBR of ^{18}F-FET uptake of 8.2±6.1 % was noted in both tumor models, which, however, appeared to be caused by a slightly increasing ^{18}F-FET uptake in the normal brain tissue. Possibly, the lower TBR of ^{11}C-MET uptake in high-grade gliomas under corticosteroid treatment reported in a previous study was caused by higher ^{11}C-MET uptake in the brain tissue, rather than lower ^{11}C-MET uptake in the tumor [21].

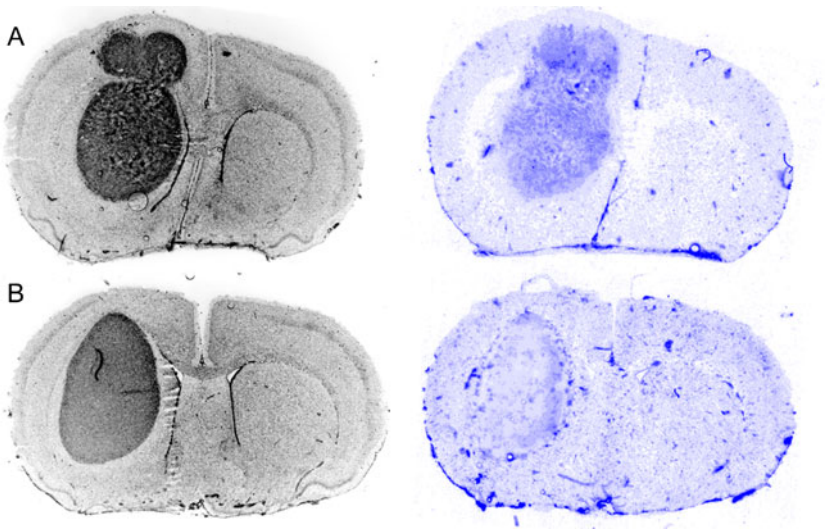

Fig. 8 Representative coronal rat brain slices of 9L gliosarcoma-bearing rats without treatment (**a**) and after Dex treatment (**b**). Histological DAPI staining is shown on the left and Evans blue fluorescence on the right. In the untreated animal, there is considerable Evans blue extravasation into the tumor, indicating a disturbed blood-tumor barrier (**a**). In contrast, after Dex treatment, Evans blue staining is considerably reduced, indicating reduced blood-tumor barrier permeability and effectiveness of Dex treatment

The mechanism for the increased ^{18}F-FET uptake in the normal brain during Dex treatment remains unclear and needs further investigation. The catabolic effects of Dex can lead to an increase of amino acid levels in the blood, which could have a stimulatory effect on amino acid uptake [37]. We consider this explanation unlikely since we observed no major effect of amino acid preloading on ^{18}F-FET uptake in the brain in additional experiments (data not shown). Another explanation may be a direct influence of Dex treatment on System L amino acid transport, which is responsible for ^{18}F-FET uptake. This hypothesis seems also unlikely, because previous experimental studies showed no significant effect of Dex on system L amino acid transport [38].

The dosage of Dex used in this experimental study is at least 4–8-fold higher than initial doses for patients with brain edema. Therefore, the observed effect of Dex on ^{18}F-FET uptake in the normal brain should be less pronounced in humans.

The effectiveness of Dex treatment in our experimental study was confirmed by the observation that Evans blue extravasation was considerably reduced in both tumor models (Fig. 8). ^{18}F-FET uptake in tumors, however, remained unchanged, despite altered BBB permeability. This finding supports the hypothesis that ^{18}F-FET uptake is not influenced by the permeability of the BBB. This aspect is still a matter of controversy although BBB disruption per se as shown by the fact that contrast enhancement in MRI, e.g. in abscesses or radionecroses, does not lead to significant ^{18}F-FET uptake [39, 40].

The results of this study are limited by the fact that animal models may not be representative for human gliomas. Furthermore, small animal PET has limitations in evaluating the tumor area, due to the finite resolution in relation to tumor size [41]. Therefore, the results need to be considered with caution, and a confirmation in human tumors is necessary.

Conclusion

The results of this experimental study indicate that TBR and the curve pattern of ^{18}F-FET uptake in gliomas are highly stable in longitudinal tests. Dex treatment induced a minor decrease of the TBR, which appears to be caused by increased ^{18}F-FET uptake in brain tissue. Tumor SUV remained constant despite a strong effect of Dex on blood-tumor barrier permeability. The results need to be confirmed in humans, but it appears that ^{18}F-FET uptake and kinetics are reliable indicators of the biological properties of cerebral gliomas, and may be helpful diagnostic parameters for monitoring of brain tumors in the course of disease.

Acknowledgments The authors wish to thank Mrs. Michaela Bohlen, Mrs. Tanja Juraschek and Mrs. Larissa Damm for animal husbandry, and Mrs. Erika Wabbals, Mrs. Silke Grafmüller and Mr. Sascha Rehbein for technical assistance in radiosynthesis of ^{18}F-FET.

Compliance with ethical standards

Conflict of interest All authors declare that they have no conflict of interest.

Ethical approval All applicable international, national, and/or institutional guidelines for the care and use of animals were followed.

References

1. Galldiks N, Langen KJ. Applications of PET imaging of neurological tumors with radiolabeled amino acids. Q J Nucl Med Mol Imaging: Off Publ Ital Assoc Nucl Med. 2015;59:70–82.
2. Herholz K, Langen KJ, Schiepers C, Mountz JM. Brain tumors. Semin Nucl Med. 2012;42:356–70.
3. Langen KJ, Hamacher K, Weckesser M, Floeth F, Stoffels G, Bauer D, et al. O-(2-[18F]fluoroethyl)-L-tyrosine: uptake mechanisms and clinical applications. Nucl Med Biol. 2006;33:287–94.
4. Wester HJ, Herz M, Weber W, Heiss P, Senekowitsch-Schmidtke R, Schwaiger M, et al. Synthesis and radiopharmacology of O-(2-[18F]fluoroethyl)-L-tyrosine for tumor imaging. J Nucl Med: Off Publ Soc Nucl Med. 1999;40:205–12.
5. Galldiks N, Langen K, Holy R, Pinkawa M, Stoffels G, Nolte K, et al. Assessment of treatment response in patients with glioblastoma using [18F]Fluoroethyl-L-Tyrosine PET in comparison to MRI. J Nucl Med: Off Publ Soc Nucl Med. 2012;53:1048–57.
6. Pauleit D, Floeth F, Hamacher K, Riemenschneider MJ, Reifenberger G, Muller HW, et al. O-(2-[18F]fluoroethyl)-L-tyrosine PET combined with MRI improves the diagnostic assessment of cerebral gliomas. Brain: J Neurol. 2005;128:678–87.
7. Pauleit D, Stoffels G, Bachofner A, Floeth FW, Sabel M, Herzog H, et al. Comparison of (18)F-FET and (18)F-FDG PET in brain tumors. Nucl Med Biol. 2009;36:779–87.
8. Pichler R, Dunzinger A, Wurm G, Pichler J, Weis S, Nussbaumer K, et al. Is there a place for FET PET in the initial evaluation of brain lesions with unknown significance? Eur J Nucl Med Mol Imaging. 2010;37:1521–8.
9. Popperl G, Gotz C, Rachinger W, Gildehaus FJ, Tonn JC, Tatsch K. Value of O-(2-[18F]fluoroethyl)- L-tyrosine PET for the diagnosis of recurrent glioma. Eur J Nucl Med Mol Imaging. 2004;31:1464–70.
10. Floeth FW, Pauleit D, Sabel M, Stoffels G, Reifenberger G, Riemenschneider MJ, et al. Prognostic value of O-(2-18F-fluoroethyl)-L-tyrosine PET and MRI in low-grade glioma. J Nucl Med: Off Publ Soc Nucl Med. 2007;48:519–27.
11. Jansen NL, Suchorska B, Wenter V, Schmid-Tannwald C, Todica A, Eigenbrod S, et al. Prognostic significance of dynamic 18F-FET PET in newly diagnosed astrocytic high-grade glioma. J Nucl Med: Off Publ Soc Nucl Med. 2015;56:9–15.
12. Popperl G, Kreth FW, Herms J, Koch W, Mehrkens JH, Gildehaus FJ, et al. Analysis of 18F-FET PET for grading of recurrent gliomas: is evaluation of uptake kinetics superior to standard methods? J Nucl Med: Off Publ Soc Nucl Med. 2006;47:393–403.
13. Weckesser M, Langen KJ, Rickert CH, Kloska S, Straeter R, Hamacher K, et al. O-(2-[18F]fluorethyl)-L-tyrosine PET in the clinical evaluation of primary brain tumours. Eur J Nucl Med Mol Imaging. 2005;32:422–9.
14. Popperl G, Kreth FW, Mehrkens JH, Herms J, Seelos K, Koch W, et al. FET PET for the evaluation of untreated gliomas: correlation of FET uptake and uptake kinetics with tumour grading. Eur J Nucl Med Mol Imaging. 2007;34:1933–42.

15. Calcagni ML, Galli G, Giordano A, Taralli S, Anile C, Niesen A, et al. Dynamic O-(2-[18F]fluoroethyl)-L-tyrosine (F-18 FET) PET for glioma grading: assessment of individual probability of malignancy. Clin Nucl Med. 2011;36:841–7.
16. Odewole OA, Oyenuga OA, Tade F, Savir-Baruch B, Nieh PT, Master V, et al. Reproducibility and reliability of anti-3-[(1)(8)F]FACBC uptake measurements in background structures and malignant lesions on follow-up PET-CT in prostate carcinoma: an exploratory analysis. Mol Imaging Biol: Off Publ Acad Mol Imaging. 2015;17:277–83.
17. Langen KJ, Roosen N, Coenen HH, Kuikka JT, Kuwert T, Herzog H, et al. Brain and brain tumor uptake of L-3-[123I]iodo-alpha-methyl tyrosine: competition with natural L-amino acids. J Nucl Med: Off Publ Soc Nucl Med. 1991;32:1225–9.
18. Piroth MD, Pinkawa M, Holy R, Klotz J, Nussen S, Stoffels G, et al. Prognostic value of early [18F]fluoroethyltyrosine positron emission tomography after radiochemotherapy in glioblastoma multiforme. Int J Radiat Oncol Biol Phys. 2011;80:176–84.
19. Kotsarini C, Griffiths PD, Wilkinson ID, Hoggard N. A systematic review of the literature on the effects of dexamethasone on the brain from in vivo human-based studies: implications for physiological brain imaging of patients with intracranial tumors. Neurosurgery. 2010;67:1799–815.
20. Sarin R, Murthy V. Medical decompressive therapy for primary and metastatic intracranial tumours. Lancet Neurol. 2003;2:357–65.
21. Herholz K, Holzer T, Bauer B, Schroder R, Voges J, Ernestus RI, et al. 11C-methionine PET for differential diagnosis of low-grade gliomas. Neurology. 1998;50:1316–22.
22. Piroth MD, Prasath J, Willuweit A, Stoffels G, Sellhaus B, van Osterhout A, et al. Uptake of O-(2-[18F]fluoroethyl)-L-tyrosine in reactive astrocytosis in the vicinity of cerebral gliomas. Nucl Med Biol. 2013;40:795–800.
23. Langen KJ, Jarosch M, Muhlensiepen H, Hamacher K, Broer S, Jansen P, et al. Comparison of fluorotyrosines and methionine uptake in F98 rat gliomas. Nucl Med Biol. 2003;30:501–8.
24. Ewing JR, Brown SL, Nagaraja TN, Bagher-Ebadian H, Paudyal R, Panda S, et al. MRI measurement of change in vascular parameters in the 9L rat cerebral tumor after dexamethasone administration. J Magn Reson Imaging: JMRI. 2008;27:1430–8.
25. Bao Q, Newport D, Chen M, Stout DB, Chatziioannou AF. Performance evaluation of the inveon dedicated PET preclinical tomograph based on the NEMA NU-4 standards. J Nucl Med: Off Publ Soc Nucl Med. 2009;50:401–8.
26. Hamacher K, Coenen HH. Efficient routine production of the 18F-labelled amino acid O-2-18F fluoroethyl-L-tyrosine. Appl Radiat Isot: Incl Data Instrum Methods Use Agric Ind Med. 2002;57:853–6.
27. Miller JN. Basic statistical methods for Analytical Chemistry. Part 2. Calibration and regression methods. A review. Analyst. 1991;116:3–14.
28. Galldiks N, Rapp M, Stoffels G, Dunkl V, Sabel M, Langen KJ. Earlier diagnosis of progressive disease during bevacizumab treatment using O-(2-18F-fluorethyl)-L-tyrosine positron emission tomography in comparison with magnetic resonance imaging. Mol Imaging. 2013;12:273–6.
29. Hutterer M, Nowosielski M, Putzer D, Waitz D, Tinkhauser G, Kostron H, et al. O-(2-18F-fluoroethyl)-L-tyrosine PET predicts failure of antiangiogenic treatment in patients with recurrent high-grade glioma. J Nucl Med: Off Publ Soc Nucl Med. 2011;52:856–64.
30. Popperl G, Goldbrunner R, Gildehaus FJ, Kreth FW, Tanner P, Holtmannspotter M, et al. O-(2-[18F]fluoroethyl)-L-tyrosine PET for monitoring the effects of convection-enhanced delivery of paclitaxel in patients with recurrent glioblastoma. Eur J Nucl Med Mol Imaging. 2005;32:1018–25.
31. Pöpperl G, Götz C, Rachinger W, Schnell O, Gildehaus FJ, Tonn JC, et al. Serial O-(2-[(18)F]fluoroethyl)-L:-tyrosine PET for monitoring the effects of intracavitary radioimmunotherapy in patients with malignant glioma. Eur J Nucl Med Mol Imaging. 2006;33:792–800.
32. Nedergaard MK, Michaelsen SR, Urup T, Broholm H, El Ali H, Poulsen HS, et al. 18F-FET MicroPET and MicroMRI for anti-VEGF and anti-PlGF response assessment in an orthotopic murine model of human glioblastoma. PLoS One. 2015;10:e0115315.
33. Nedergaard MK, Kristoffersen K, Michaelsen SR, Madsen J, Poulsen HS, Stockhausen MT, et al. The use of longitudinal 18F-FET MicroPET imaging to evaluate response to irinotecan in orthotopic human glioblastoma multiforme xenografts. PLoS One. 2014;9:e100009.
34. Galldiks N, Stoffels G, Ruge MI, Rapp M, Sabel M, Reifenberger G, et al. Role of O-(2-18F-fluoroethyl)-L-tyrosine PET as a diagnostic tool for detection of malignant progression in patients with low-grade glioma. J Nucl Med: Off Publ Soc Nucl Med. 2013;54:2046–54.
35. Jansen NL, Suchorska B, Schwarz SB, Eigenbrod S, Lutz J, Graute V, et al. [18F]fluoroethyltyrosine-positron emission tomography-based therapy monitoring after stereotactic iodine-125 brachytherapy in patients with recurrent high-grade glioma. Mol Imaging. 2013;12:137–47.
36. Habermeier A, Graf J, Sandhofer BF, Boissel JP, Roesch F, Closs EI. System L amino acid transporter LAT1 accumulates O-(2-fluoroethyl)-L-tyrosine (FET). Amino Acids. 2015;47:335–44.
37. Lahoutte T, Caveliers V, Franken PR, Bossuyt A, Mertens J, Everaert H. Increased tumor uptake of 3-(123)I-Iodo-L-alpha-methyltyrosine after preloading with amino acids: an in vivo animal imaging study. J Nucl Med: Off Publ Soc Nucl Med. 2002;43:1201–6.
38. Le Cam A, Freychet P. Effect of glucocorticoids on amino acid transport in isolated rat hepatocytes. Mol Cell Endocrinol. 1977;9:205–14.
39. Hutterer M, Nowosielski M, Putzer D, Jansen NL, Seiz M, Schocke M, et al. [F-18]-fluoro-ethyl-L-tyrosine PET: a valuable diagnostic tool in neuro-oncology, but not all that glitters is glioma. Neuro-Oncology. 2013;15:341–51.
40. Langen KJ, Galldiks N. Reply to "[18F]-fluoro-ethyl-L-tyrosine PET: a valuable diagnostic tool in neuro-oncology, but not all that glitters is glioma" by Hutterer et al. Neuro-Oncology. 2013;15:816–7.
41. Christian N, Lee JA, Bol A, De Bast M, Jordan B, Gregoire V. The limitation of PET imaging for biological adaptive-IMRT assessed in animal models. Radiother Oncol: J Eur Soc Ther Radiol Oncol. 2009;91:101–6.